ORIGINAL RESEARCH PAPER

Synthesize and characterization of hollow and core/shell based on CeO_2 as a alcohol sensor

Zahra Rasouli [1], Mohammad Yousefi [1]*, Susan Samadi [2], Khadijeh Kalateh [2], Maryam Bikhof Torbati [2]

[1] Department of Chemistry, Science and Research Branch, Islamic Azad University, Tehran, Iran
[2] Department of Chemistry, College of Basic Science, Yadegar-e-Imam Khomeini (RAH) Shahr-e-Rey Branch, Islamic Azad University, Tehran, Iran

Received: 2017-08-02 Accepted: 2017-09-29 Published: 2017-12-20

ABSTRACT
In this study, CeO_2 hollow spherical nanoparticles, CeO_2/SiO_2 @ CeO_2 core/shell composites, and hollow CeO_2/SiO_2 sensors were synthesized and their microstructures were researched by FT-IR, XRD, FESEM, EDX and BET analyses. The peaks observed in the FT-IR spectra of the synthesized samples corresponded to Ce-O stretching vibration (ca. 566 cm^{-1}) and O-Si-O bending vibration (ca. 470 cm^{-1}). XRD diffraction patterns showed peaks at 2θ values in the 28.95° , 33.74°, 47.75° , 57.04°, 59.52° ,and 69.4° confirming cubic phase of CeO_2. The FESEM images showed that the particle shape was approximately spherical. The results of BET showed that, surface area of the CeO_2 hollow spherical nanoparticles, CeO_2/SiO_2 @ CeO_2 and hollow CeO_2/SiO_2 core/shell particles were 102.78, 80.49, and 119.71 m^2/g, respectively. The nanosized metal oxides were used to quantitatively and qualitatively identify 1-propanol, 2-propanol, ethanol and methanol. The results showed that, the hollow CeO_2/SiO_2 core/shell was of larger potentials for qualitative identification of 1-propanol and quantitative measurement of 2 -propanol and ethanol.

Keywords: *Cerium dioxide, Core/Shell, Hollow, Sensor, Volatile organic compounds*

How to cite this article
Rasouli Z, Yousefi M, Samadi S, Kalateh Kh, B. Torbati M. Synthesize and Characterization of Hollow and Core/Shell Based on CeO_2 as a Alcohol Aensor. J. Nanoanalysis., 2017; 4(4): 280-289. DOI: 10.22034/jna.2017.539993

INTRODUCTION

Recently, environmental protection has gained much attention due to the widespread emission of gas contaminants. Harmful volatile organic substances,including 1-propanol, 2-propanol, and ethanol are of special importance due to the associated problems with them such as wackiness, drowsiness, headache, nausea, anesthesia, respiratory depression, and central nervous system disorders [1, 2]. Therefore, extensive research has been done on the development and enhancement of sensitivity and efficiency of gas sensors. Among the various gas sensors, metal oxide conductors have been widely considered. These were first introduced by Seiyama *et al.* in 1962 and later on commercializing by Naoyoshi Taguchi. These sensors have been used to identify several toxic and hazardous gases because of their simple sensory mechanism, low maintenance cost, small size, superior performance, and ease of use. In addition

* Corresponding Author Email: myousefi50@hotmail.com

to the advantages mentioned, these sensors suffer from limitations in terms of performance at elevated temperatures and poor selectivity [3]. Numerous strategies have been proposed to overcome these disadvantages. Among these strategies, core/shell and hollow structures are used to measure different types of materials, such as moisture, ethanol, hydrogen, ammonia, propane, carbon dioxide, etc. [2-11]. Hollow structures have many applications in different areas (e.g. gas sensors) due to their low density, well-defined morphology, large surface area, high load bearing capacity, free space, large size, uniform geometry, and high permeability. [12-15]. Studies have shown that, morphology, particle size, structure, chemical composition and form significantly affect the efficiency of gas sensors [11]. Among the core/shell sensors, cerium dioxide-based ones have attracted particular attention. In recent years, cerium has been made to various morphologies including nanoparticles, nanofibers, nanowires, nanotubes, hollow spherical particles, and so on [12, 16]. CeO_2 is of special properties such as high oxygen storage capacity, which ends up storing plenty of oxygen particles and reducing the potential for reduction between Ce^{3+} and Ce^{4+}, making CeO_2 a good candidate gas sensor. Cerium dioxide is a key factor in the development of sensory properties, because it is a strong receiver in the core/shell state wherein an electron drainage layer is created near its semiconductive surface; furthermore, the ability of cerium to rapidly create oxygen vacancy makes it possible to repeat Ce^{3+}/Ce^{4+} cycle [17-20]. Cerium dioxide is used alone, doped in the form of core/shell compounds with polymers and other metal oxides, and as a composite with metals for the detection of various gases such as ammonia [6], ethanol [20, 21], moisture [22], carbon dioxide [11], carbon monoxide [23, 24], nitrogen dioxide and hydrogen [24]. Moreover, SiO_2 alone has been used as an alcohol sensor [25, 26].

Despite the studies done in this area, to the best of our knowledge, very little is known on hollow CeO_2 alone and hollow CeO_2/SiO_2 core/shell composites as gas sensor.

In this study, different composites of cerium (CeO_2 hollow spherical nanoparticles, core/shell compounds, CeO_2/SiO_2 @ CeO_2, and hollow CeO_2/SiO_2) were prepared. The synthesized compounds were identified using FT-IR, XRD, FESEM, and BET analyses, with their performance in detecting volatile organic compounds (VOCs) (e.g. 1-propanol, 2- propanol, ethanol, and methanol) been evaluated.

EXPERIMENTAL

Materials and characterization

All chemicals used in the present research were analytic reagents (AR) including Ce $(NO_3)_3.6H_2O$, ultra pure), tetraethyl ortho-silicate TEOS, D (+) - glucose monohydrate, ethanol absolute, NH_4OH, $NH_4Ac.2H_2O$, 1-propanol (procured from Merck Company), 2-propanol, ethanol, methanol (procured from Romil Company), and distilled water.

FT-IR spectra of samples were recorded using NEXUS 870 (USA) on KBr disks, and crystalline structures of the samples were evaluated by X-ray diffraction (XRD) analysis on a 3003 PTSSEIERT (Germany). Morphology and composition of the samples were analyzed using FESEM and EDX analyses (Tescan, MIRA3, Hitachi S4160), while specific surface area (BET) was determined on a Belsorp Mini (II) (Japan).

Synthesis of sensors

Synthesis of templates

In this stage, firstly 8 g of D-(+) glucose monohydrate was dissolved in 30 ml of water, and the obtained clear solution was transferred into a 100 ml autoclave where it was heated at 160° C for 22 hours until a black precipitate, namely carbon spheres template, was obtained. The sediments were then washed with distilled water and ethanol and then dried at 80°C.

Synthesis of hollow CeO_2 sensor

In order to synthesize this sensor, ammonium acetate ($NH_4Ac.2H_2O$) and cerium nitrate (Ce $(NO_3)_3.6H_2O$) were mixed at a molar ratio of 6:1 in 20 ml of absolute alcohol followed by the dispersion of 0.2 g of as-prepared carbon spheres. The resulting mixture was transferred into a 100 ml-autoclave where it was heated at 180°C for 6 hours. Afterwards, precipitates (C–Ce $(OH)_3$) were separated from the mixture by centrifugation. The precipitates were dried at 100°C for 6 hours,followed by heating at 510°C for 6 hours, so as to obtain a lemon-yellow powder designated as Sensor S_1.

Synthesis of hollow CeO_2/SiO_2 sensor

This type of sensor was synthesized in two different ways.

A: CeO_2/SiO_2 @ CeO_2 sensor

The C-$Ce(OH)_3$ prepared in previous section was mixed with tetraethyl ortho-silicate (TEOS), 25% ammonia, and absolute alcohol at a C-$Ce(OH)_3$:TEOS molar ratio of 1:7; the solution was then subjected to ultrasonic dispersion before being transferred to a Teflon autoclave where it was heated at 180°C for 10 hours.

The resulting sediments were centrifuged and heated to 600 °C from ambient temperature with a temperature ramp of 5 °C min^{-1} and kept at the same temperature for 3 h in a furnace under argon atmosphere and designated as Sensor S_2.

B: Hollow CeO_2/SiO_2 sensor

Following the same procedure as that in Section A, hollow CeO_2, rather than C-Ce $(OH)_3$ was synthesized and designated as Sensor S_3.

About 5 mg of sensors were used to determine volatile organic compounds (VOCs) such as 1-propanol, 2- propanol, ethanol, and methanol both quantitatively and qualitatively.

Gas identification system

In this study, the sensor system consists of three parts: gas intake, injection chamber, and sensor. Gas intake heats the carrier gas to 100°C, so as to keep it from being liquefied in contact with the evaporated alcoholic sample. The flow rates of the vapor were adjusted in 100 ml/min. The injection chamber is composed of two parts, a part where the sample is injected and evaporated by heating, and another one which serves as control. The sample gas is finally sent to the third part, sensor, which consists of two parts and measures the changes in the resistance of alcohol vapors, so as to control the unit to eliminate environmental effects.

The sensor response is defined as the following equation [3].

Where:
Rs=(Ra/Rg)
Rs=Sensor response
Ra=Sensor resistance in the air
Rg=Sensor resistance in target gas

The response and recovery times are defined as the times by which the sensor achieves 90% of the total voltage change in the case of adsorption and desorption processes, respectively [2].

A general schema of the sensor and associated electrical circuit is shown in Fig. 1. The circuit was fed with a constant voltage (V=5) which was monitored using a recording device. The following equation expresses the relationship between measured Vs voltage and the sensor sensitivity:

Rs=Ra/Rg=Vs/ V-Vs

The system was used to study 1-propanol, 2-propanol, ethanol, and methanol gases.

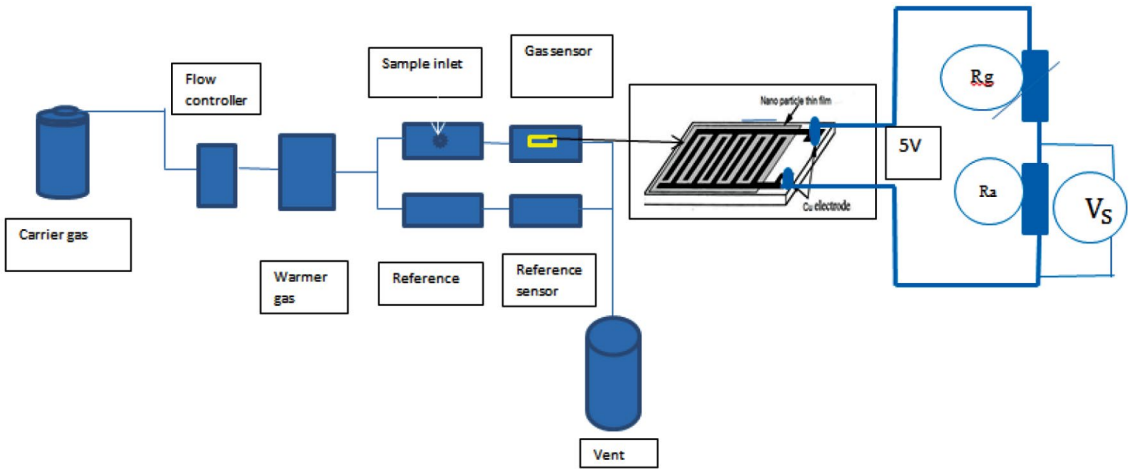

Fig. 1. General schema of the sensor.

RESULTS AND DISCUSSION

Identification of sensor structure

The FT-IR spectra of sensor S_1- S_3 are shown in Fig. 2.

The peaks corresponding to Ce=O terminal stretching (ca. 1400 cm^{-1}) and Ce – O stretching vibration,(ca. 566 cm^{-1}) are too weak (Figs. 2a-2c). Also in Fig. 2, the peaks at ca. 3440 cm^{-1} and 1650 cm^{-1} are attributed to water molecules. The sharp strips in Figs. 2b, 2c at 1082 cm^{-1} refer to Si-O-Si asymmetric stretching. The strips at 814 cm^{-1} and 470 cm^{-1} are attributed to Si-O-Si symmetric stretching and O-Si-O bending vibration, respectively [13, 27, 28].

Crystalline phases of Sensors S_1, S_2, and S_3 were identified by XRD analysis (Figs. 3a-3c, respectively). On the XRD patterns, the peaks at 2θ values of 28.95°, 33.74°, 47.75°, 57.04° 59.52°, and 69.4° are related to planes (111), (200), (220), (311), (222) and (400), respectively, representing the face-centered cubic phase of CeO_2 (matched to the card JCPDS 0349-34)[13,27]. In addition, Figs. 3b, 3c showed a wide weak peak located at 23°, which should be attributed to amorphous SiO_2 [13,28].

Fig. 4 shows FESEM images of the samples. Morphology of Sensor S_1 (Fig. 4 a) shows that the spherical particles are nanosized and the particle size distribution is narrow. Fig. 4b shows the morphology of Sensor S_2, where spherical particles are of micro size and particle size distribution is wide.

Fig. 4c shows the morphology of Sensor S_3, indicating spherical particles of nano size and narrow size distribution in a porous matrix.

As it can be seen, the size of the CeO_2 particles has become smaller when those were coated with SiO_2, possibly because SiO_2 prevented size distribution of the CeO_2 particles from being widened and hindered mass transfer, resulting in smaller core/shell particle size. Similar results are reported elsewhere [29].

EDX analysis results are shown in Figs. 5a-5c. There are Ce and O elements in all samples, and Si is present only in Figs. 5b, 5c. Aiming at absorbing the target gas, surface area of sensor is important. Therefore, BET tests were performed on Sensors S_1- S_3. The results are shown in Table 1. According to the results, Sensors S_3 and S_2 corresponded to the largest and smallest surface areas, respectively. The maximum total pore volume of the vent was obtained for Sensor S_3, and the maximum mean pore diameter was that of Sensor S_2. Therefore, it was found that, hollow structure affects the specific surface area of the synthesized sensor.

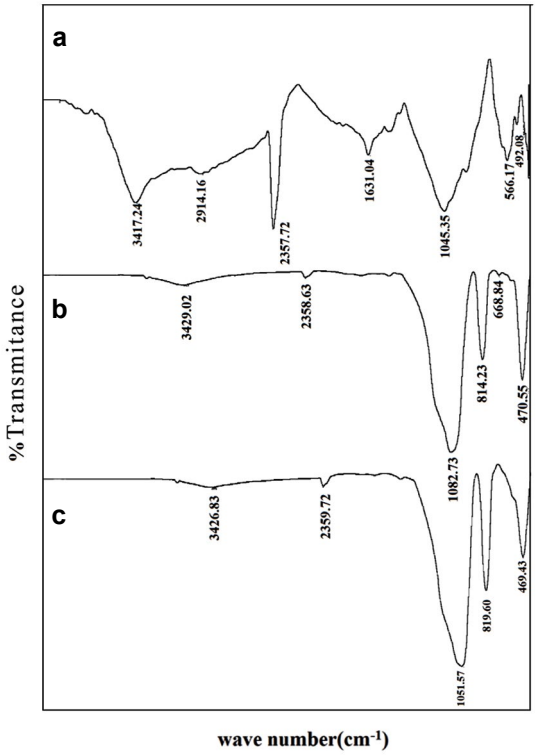

Fig. 2. The FT-IR spectra of Sensors a) S_1, b) S_2 and c) S_3.

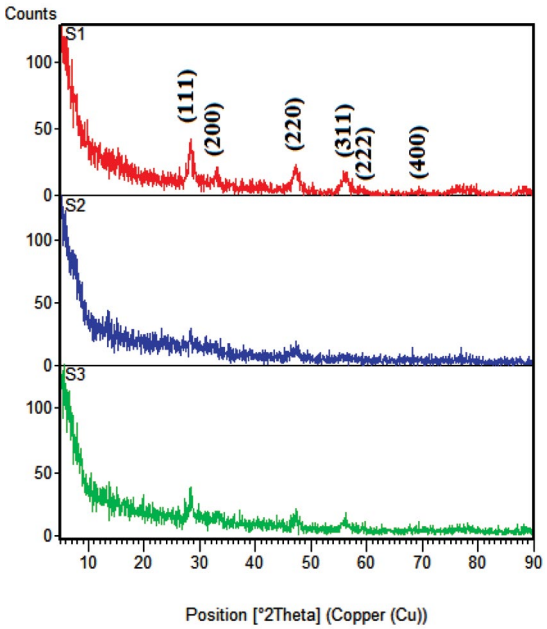

Fig. 3. The XRD patterns of Sensors a) S_1, b) S_2 and c) S_3.

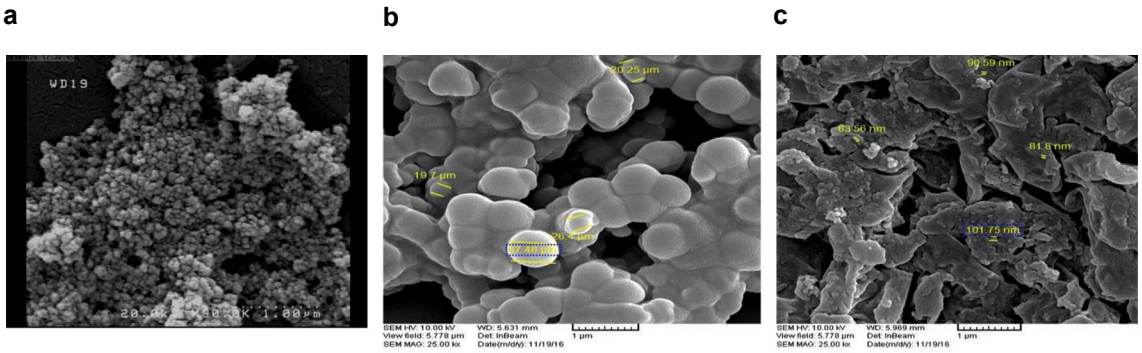

Fig. 4. The FESEM images of Sensors a) S_1, b) S_2 and c) S_3.

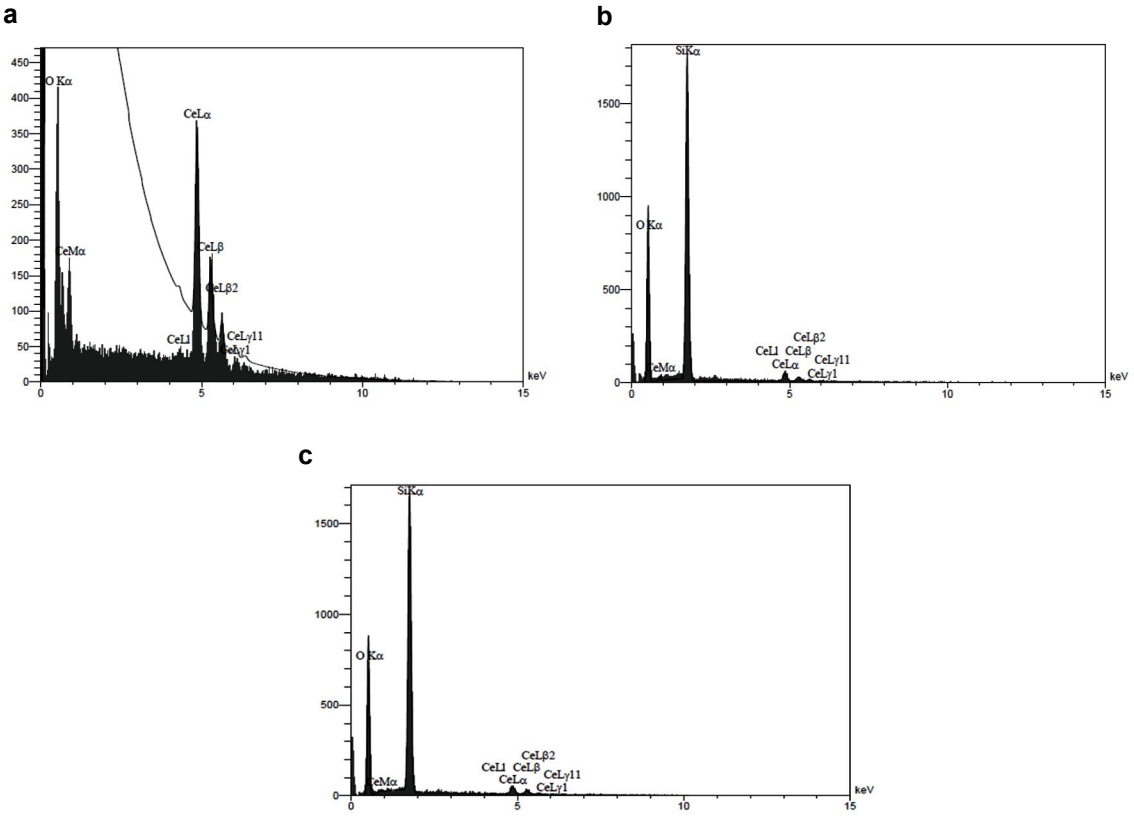

Fig. 5. The EDX analysis of Sensors a) S_1, b) S_2 and c) S_3.

Table 1. $a_{s,}$ BET , Total pore volume and Mean pore diameter of sensors

Sample	$a_{s,\,BET}$ (m^2/g)	Total pore volume (cm^3/g)	Mean pore diameter (nm)
S_1	102.78	0.090218	3.5111
S_2	80.49	0.6414	31.88
S_3	119.71	0.8261	27.603

Sensor performance

Sensitivities of the synthesized sensors were investigated on four alcoholic samples, namely 1-propanol, 2-propanol, ethanol, and methanol, at 350 ppm. The results in Figs. 6-8 show that, all sensors exhibited very little sensitivity to methanol, but different sensitivities were observed for other samples.

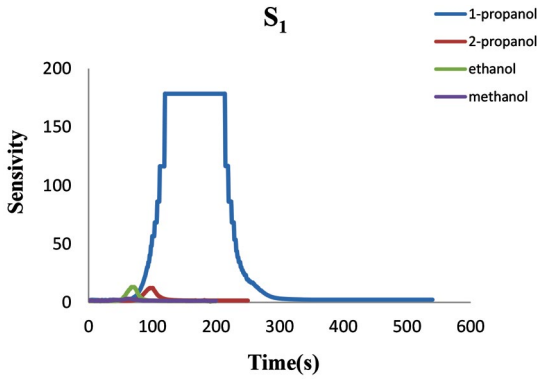

Fig. 6. The Sensitivities of S_1 on four alcoholic samples.

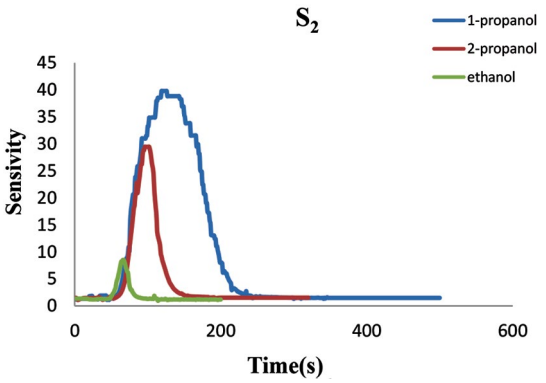

Fig. 7. The Sensitivities of S_2 on four alcoholic samples.

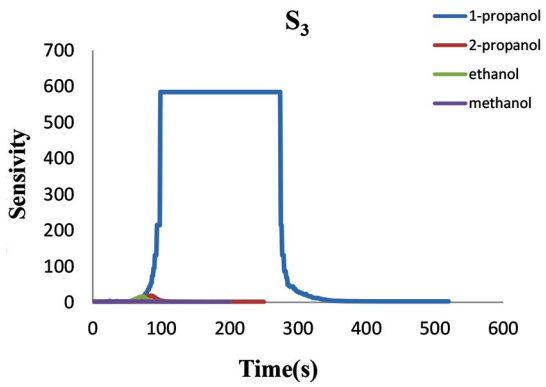

Fig. 8. The sensitivities of S_3 on four alcoholic samples.

Sensor S_3 was seen to be highly sensitive to 1-propanol, i.e. it was selective toward 1-propanol and could serve as an excellent sensor for detecting 1-propanol. In order to quantitatively study how sensitive was each sensor to volatile organic compounds, it was tested to evaluate sample gases at 50-600 ppm. The results in Figs. 9-11 show that, the sensitivity increases with gas concentration. Figs. 9-11 show variations in sensitivity of the sensors to 1-propanol. Ideally, sensor response is linearly related to the measured gas concentration. This relation is approximated as the following empirical relationship where C_{gas} is the target gas concentration, β is a factor ideally ranging between 0.5 and 1, and α is a coefficient [18].

$$\text{Response}=1+\alpha C_{gas}^{\beta}$$

Logarithms of the sensitivity of each sensor to different concentrations of each sample were compared (Table 2). According to the R^2 values in Table 2, different linear correlations are observed between sensor response and gas concentration. Sensor S_1 showed the best correlation (R^2 =0.9779) in detecting 1-propanol. Therefore, it can be used for quantitative measurement of 1-propanol.

With R^2 =0.94, Sensor S_3 had similar conditions relative to 2-propanol and ethanol, making capable of quantitatively measuring these two samples. The response and recovery times are among important and operational parameters of a gas sensor: the lower the values of these parameters, the better, i.e. the sensor can give successive and independent responses to stimulate. Table 3 reports response and recovery times for Sensors S_1 to S_3. Based on the information in Table 3, response and recovery times of all of the sensors given were evaluated as appropriate. The lowest response and recovery times were those of Sensors S_1 and S_3 to methanol, respectively.

Repeatability of responses is very important in practical use of sensors. Sensor accuracy is defined as the proximity of two or more measurements performed under the same conditions. The higher the accuracy, the more concentrated the standard deviation of the dispersion around the actual value. Relative standard deviation (RSD %) is an indicator of accuracy.

To evaluate this parameter,the sensitivity of each sensor to VOCs at 350 ppm was measured four times. Table 4 shows the obtained values of RSD% of sensors responses to VOCs. As indicated in the table, all of the sensors were seen to be appropriately sensitive to different samples. High sensitivity of the

sensors to 1-propanel indicated adequate repeatability of the sensor measurements. Repeatability of sensor S_2 for methanol detection is not reported since it exhibited no sensitivity to methanol.

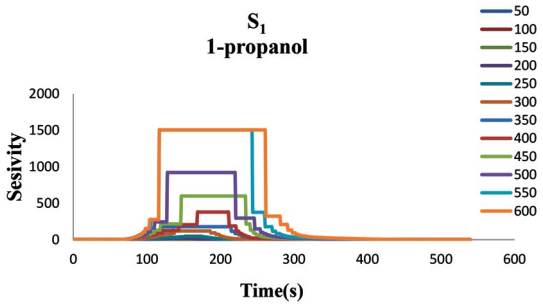

Fig. 9. The variations in sensitivity of S_1 to 1-propanol at 50-600 ppm.

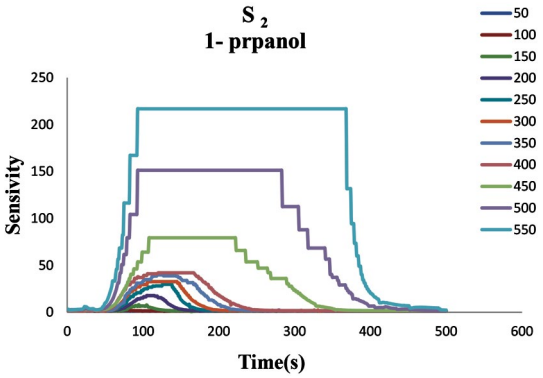

Fig. 10. The variations in sensitivity of S_2 to 1-propanol at 50-600 ppm.

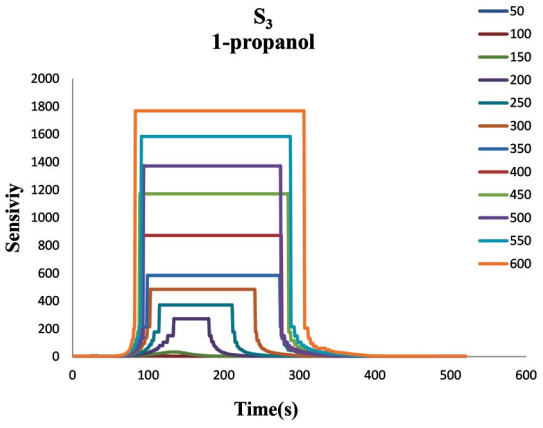

Fig. 11. The variations in sensitivity of S_3 to 1-propanol at 50-600 ppm.

Gas sensing mechanism

In a semiconductor sensor, concentration measurement mechanism is based on changes in the resistance of the sensitive layer on the sensor. In other words, when the sensor is placed in the pure air, its resistance increases; while it has its resistance reduced when exposed to a reducing gas (such as an organic volatile liquid) [30]. The gas sensing mechanism usually consists of two steps: (1) the gas spreads on the sensor, and (2) the gas reacts with the surface sensor. It should be noted that, the gas diffusion rate differs according to the Knudsen (D_k) diffusion constant:

$$D_k=3r/4\ \sqrt{(2RT/\pi M)}$$

Where r is the radius of the pore, M is the molecular mass, and T is temperature. As the relationship shows, the greater the pore radius, high operating temperature and lower molecular mass lead to a high the gas diffusion rate [31].

When the sensor is exposed to air, the following reactions may occur on the sensor in terms of temperature.

$$O_2\ (gas) \rightarrow O_2\ (ads) \quad (1)$$

$$O_2\ (ads) + e^- \rightarrow O_2^-\ (ads) \quad (2)$$

$$O_2^-\ (ads) + e^- \rightarrow 2O^-\ (ads) \quad (3)$$

$$O^-\ (ads) + e^- \rightarrow O^{2-}\ (ads) \quad (4)$$

Reaction 2 happens in temperature ranges 25-150°C and 3, 4 above 150°C [30, 31, 32]. Due to the use of sensors manufactured at ambient temperature, reaction 2 is likely to contribute to their mechanism of working.

In metal oxides, oxygen is absorbed on an active sensor surface in the vicinity of the sample, so that a change is observed in the absorbing oxygen balance. As a result, chemical absorption is recorded as a change in the sensor resistance [33].

According to the following equations, tested VOCs could be transformed into water and carbon dioxide. [2, 34]

$$C_2H_5OH + 3O_2^- \rightarrow 2CO_2 + 3H_2O + 3e^-$$

$$2C_3H_7OH + 9O_2^- \rightarrow 6CO_2 + 8H_2O + 9e^-$$

The BET showed, the specific surface area of

hollow CeO_2 is 102.78 m^2/g. In this research, we used two different methods for synthesis core/shell sensors. In which case that, SiO_2 was ensconced on the ceria particles and then carbon omitted (S_2), the specific surface area reduced to 80.49 m^2/g which it can be attributed to prevention of the SiO_2 shell from escape carbon. In the other words, amount of access to hollow CeO_2 reduces in this method and sizes of resultant particles were large, in the average size 29.45µm. In S_3 sensor, the first central carbon omitted and then SiO_2 shell was covered hollow CeO_2.Evidently, the specific surface area was increased regard to S_2 sensor and reached to119.71 m^2/g. In this state, the maximum surface area and total pore volume were obtained.

According to explained mechanism, air contact surface or target gases with constructing nanomaterial caused changes in resistance and sensivity. Therefore, whatever the specific surface area increases, sensor sensitivity is expected to improve as well. These prediction and mechanism is quite confirmed for the two target gases of ethanol and 1-propanol. But there is a different behavior with 2- propanol despite lower surface area. It means despite lower surface area , S_2 has more sensitivity than S_3. In this regard, can be referred to branched form 2-propanol and spatial inhibition in its surface absorption on the sensor. However, it is important to note that apart from the specific surface area of the cavities, average size of cavities can also affect the sensitivity. S_2 has the highest average diameter of the cavity (31.88 nm). Therefore, the 2-propanol despite of branching and spatial inhibition, can be absorbed on the sensor's surface more comfortable than the S_3 sensor, and changes its resistance. So is seen more sensitivity.

Table 2. Related line equations via sample different concentrations

Material	S_1		S_2	
	Equation	R- squared	Equation	R- squared
1-Propanol	Y=0.0061x+0.0084	0.9779	Y=0.0038x+0.2893	0.9481
2-Propanol	Y=0.0055x-0.6174	0.8951	Y=0.0034x-0.0755	0.9158
Ethanol	Y=0.0047x-0.4873	0.9448	Y=0.0035x-0.3118	0.9338
Methanol	Y=0.0029x-0.3014	0.7924	-	-

Material	S_3	
	Equation	R- squared
1-Propanol	Y=0.0048x+0.8346	0.8047
2-Propanol	Y=0.004x-0.2967	0.9569
Ethanol	Y=0.0035x-0.2576	0.9402
Methanol	Y=0.0022x-0.2195	0.8336

Table 3. The response and recovery times for different samples

Material	S_1		S_2		S_3	
	Response Time(s)	Recovery Time(s)	Response Time(s)	Recovery Time(s)	Response Time(s)	Recovery Time(s)
1-Propanol	90	135	73	148	68	246
2-Propanol	61	66	60	85	48	119
Ethanol	35	79	31	48	37	88
Methanol	4	57	-	-	18	34

Table 4. The RSD% of sensors sensitivity for different samples

Material	S_1		S_2		S_3	
	RSD%	[a]A.R.V	RSD%	A.R.V	RSD%	A.R.V
1-Propanol	0.72	177.98	4.17	35.72	0.408	582.17
2-Propanol	1.16	13.12	4.26	30.87	2.49	17.85
Ethanol	12.64	13.28	31.81	13.025	6.94	15.51
Methanol	0.87	3.05	-	-	0.17	2.19

[a]A.R.V Average Response Value.

CONCLUSION

In this study, three cerium-based gas sensors were manufactured, including CeO_2 hollow spherical nanoparticles, and core/shell composites including CeO_2/SiO_2 @ CeO_2, and hollow $CeO_{2/}SiO_2$, using solvothermal method. The synthesized sensors were used to identify 1-propanol, 2-propanol, ethanol, and methanol, both quantitatively and qualitatively. The results showed that, sensor S_3 had the highest sensitivity to 1-propanol, so that it could be used to identify this sample qualitatively. The sensor further showed very good sensitivity to changes in the concentration of 2-propanol and ethanol, confirming its applicability for quantitative measurement of these gases. This high sensitivity could be explained by large specific surface area and pore size. Indeed, an increase in specific surface area would have a positive effect on sensitivity of the sensor. While an increase in the porosity and size of cavities of the nanostructured sensor had positive effects on the sensitivity and response time; these can be attributed to quicker and more convenient absorption of the gas sample on the surface of such a sensor, which is consistent with Knudsen's relationship and the results reported by Simon [33].

ACKNOWLEDGMENTS

This study was supported by the Science and Research Branch, Islamic Azad University.

CONFLICT OF INTEREST

The authors declare that there is no conflict of interests regarding the publication of this manuscript.

REFERENCES

1. M. Vujasinović, M .Kočar, K .Kramer, M .Bunc, and M. Brvar, Human and Experimental Toxicology, 26, 975 (2007).
2. M. Poloju, N. Jayababu, E. Manikandan, M.V. Ramana Reddy, Journal of Materials Chemistry C, (2017), DOI: 10.1039/C6TC05095F.
3. M. M. Sanjit., R.Prabhakar, and Y.T. Yu., ACS Appl. Mater. Interfaces, 7, 9462 (2015).
4. Y. Zhao, Y. Ding, X.Chen, W. Yang , Sensors and Actuators B, 203, 122 (2014).
5. X. Lai, J. Li, B.A. Korgel, Z. Dong, Z. Li, F. Su, J. Du, and D. Wang, Angew. Chem., 123, 2790 (2011).
6. L. Wang, H.Huang, S. Xiao, D. Cai, Y. Liu, B. Liu, D.Wang, C. Wang, H. Li, Y. Wang, Q.Li, and T.Wang, ACS Appl. Mater. Interfaces, 6, 14131 (2014).
7. X.J. Chen, J. Zhang, D. F. Ma, S. C. Hui, Y. L. Liu, W.Yao, Journal of Applied Polymer Science , 121, 1685 (2011) .
8. S. Das, S. Sinha, B. Das, S. K. Suar , S. K. S. Parashar , M. Mohapatra, A. Mishra, S.K. Tripathy, J Mater Sci: Mater Electron, 25, 217 (2014).
9. Kewei Liu , Makoto Sakurai , and Masakazu Aono, small (2012), DOI: 10.1002/smll.201201028.
10. Y.-J. Chen, C. L. Zhu, L.J. Wang, P. Gao, M.S. Cao and X.L. Shi, Nanotechnology, 20, 045502 (2009).
11. E. Laubender, N.B. Tanvir, O. Yurchenko, G. Urban, Procedia Engineering, 120, 1058 (2015).
12. J. Zhang, M.Gong, C. Tian, C.A. Wang, DOI: http://dx.doi.org/10.1016/j.ceramint.2015.12.166
13. Y. Sun, L. Zhang, Y. Wang, P.Chen, S. Xin, H. Jiu, J. Liu, Journal of Alloys and Compounds, 586, 441 (2014).
14. J. Liu, M. Dai, T.Wang, P.Sun, X.Liang, G. Lu, K. Shimanoe, and N. Yamazoe, ACS Appl. Mater. Interfaces February 24, (2016), DOI: 10.1021/acsami.6b00169.
15. Z. Li, F. Han, C. Li, X.Jiao and D. Chen , RSC Adv., 6, 60975 (2016).
16. S. Wang, J.Zhang, J. Jiang, R. Liu, B. Zhu, M. Xu, Y. Wang, J. Cao, M. Li, Z. Yuan, S.Zhang, W. Huang, S. Wu, Microporous and Mesoporous Materials, 123, 349 (2009).
17. Z. Wang, S. Jiang, Y. Li, P.Xu, K.Zhao, L.Zong, H.Wang and R. Yu, Science China Press and Springer-Verlag Berlin Heidelberg (2017), DOI: 10.1007/s40843-017-9042-0.
18. W. Qin, L. Xu, J.Song, R. Xing, H.Song, Sensors and Actuators B, 185, 231 (2013).

19. K.Ma, W. Zou, L.Zhang, L.Li, S.Yu, C. Tang, F. Gao and L.Dong , RSC Adv., 7, 5989 (2017).
20. Y.J. Chen, G. Xiao, T.S. Wang, F. Zhang, Y. Ma, P. Gao, Sensors and Actuators B, 156, 867 (2011).
21. S. Yan,S. Ma, X.Xu, Y. Lu, H. Bian, X.Liang, W. Jin, H.Yang, Materials Letters, 165, 9 (2016).
22. X .Q .Fu, C. Wang, H. C. Yu, Y. G. Wang, and T. H .Wang, Nanotechnology ,18, 145503 (2007).
23. L. Liao, H. X. Mai, Q. Yuan, H. B. Lu, J. C. Li, C. Liu, C. H. Yan, Z. X. Shen, and T. Yu, J. Phys. Chem. C, 112, 9061 (2008).
24. N. A. Joy, M.I. Nandasiri, P.H. Rogers, W. Jiang, T. Varga,S. V. N. T. Kuchibhatla, S.Thevuthasan, and M. A. Carpenter, Anal. Chem., 84, 5025 (2012).
25. N.A. Beckersa, M.T. Taschuka, M.J. Bret, Sensors and Actuators B ,176 ,1096 (2013).
26. P. Innocenzi, A.Martucci, M. Guglielmi, A. Bearzotti, E. Traversa, J. C. Pivin, Journal of the European Ceramic Society ,21, 1985 (2001).
27. Lixin Zhang,Jia Zhang,Hongfang Jiu,Xia Zhang,Meiling Xu, J Mater Sci,(2015), DOI 10.1007/s10853-015-9070-5.
28. A.K. Bhosale, P.S.Shinde, N.L.Tarwal, P.M.Kadam, S.S.Mali, P.S.Patil, Solar Energy Materials & Solar Cells, 94, 781 (2010).
29. J. Mao ,Y. Bai ,L.Gu, Peter A., v.Aken ,M. J. Tu, J Nanopart Res, 12, 2045 (2010).
30. A.Mirzaei, K. Janghorban, B.Hashemi, A.Bonavita, M. Bonyani, S. G. Leonardi and G. Neri, Synthesis, Nanomaterials, 5, 737 (2015).
31. W. Li, S.Ma, Y. Li, G. Yang, Y. Mao, J. Luo, D. Gengzang,X. Xu, S. Yan, Sensors and Actuators B 211, 392 (2015).
32. M.Li, H. Zhu, J. Cheng, M. Zhao, W.Yan, J Porous Mater, Volume 24, Issue 2, 507 (2017).
33. M. E. Franke, T. J. Koplin, and U. Simon, small, 2, No. 1, 36 (2006).
34. C. M. Hung, N. D. Hoa, N.V. Duy, N. V.Toan, D. T.T.Le, N. V.Hieu, Journal of Science: Advanced Materials and Devices 1, 45e50(2016).
35. Andrew J. Burris,Kelvin Tran,Quan Cheng, J. Anal. Test., (2017), DOI 10.1007/s41664-017-0012-x.
36. Chengjun Dong, Xinxin Xing, Nan Chen, Xu Liu, Yude Wang, Sensors and Actuators B 230, 1 (2016).
37. Sungryul Yun, Jaehwan Kim, Sensors and Actuators B 150, 308 (2010).
38. Jack Lombardi, Mark D. Poliks, Wei Zhao, Shan Yan, Ning Kang, Jing Li, Jin Luo, Chuan-Jian Zhong, Ziang Pan, Mihdhar Almihdhar, Benjamin S. Hsiao, IEEE 67th Electronic Components and Technology Conference (2017).